European Journal of Nuclear Medicine and Molecular Imaging (2019) 46:396–406
https://doi.org/10.1007/s00259-018-4119-8

ORIGINAL ARTICLE

Quantifying SV2A density and drug occupancy in the human brain using [^{11}C]UCB-J PET imaging and subcortical white matter as reference tissue

Michel Koole[1] · June van Aalst[1] · Martijn Devrome[1] · Nathalie Mertens[1] · Kim Serdons[1] · Brigitte Lacroix[2] · Joel Mercier[2] · David Sciberras[2] · Paul Maguire[2] · Koen Van Laere[1]

Received: 9 May 2018 / Accepted: 30 July 2018 / Published online: 18 August 2018

Abstract

Purpose A [^{11}C]UCB-J blocking study was performed in healthy volunteers to validate simplified, non-invasive measures for quantifying presynaptic SV2A expression using subcortical white matter as reference tissue.

Methods Ninety minutes dynamic [^{11}C]UCB-J PET scanning with arterial blood sampling was performed in 10 healthy volunteers (8 M/2F; age 27.6 ± 10.0 yrs), before and after administration of a novel chemical entity with selective affinity for SV2A. The centrum semi-ovale (SO) was validated as reference region by comparing baseline and post treatment distribution volume (V_T). Using SO as reference tissue, Binding Potential (BP_{SO}) using a Simplified Reference Tissue Model (SRTM, down to 60 min acquisition) and Standardized Uptake Value Ratios (60-90 min post injection - $SUVR_{SO,60\text{-}90min}$) were compared with regional distribution volume ratios (DVR). Next, SV2A occupancy values based on SRTM BP_{SO} and $SUVR_{SO,60\text{-}90min}$ were compared to occupancy estimates using regional V_T values and a Lassen plot.

Results After pretreatment, regional V_T values were reduced significantly except for SO. Highly significant correlations were found between DVR, SRTM BP_{SO} and $SUVR_{SO,60–90min}$. Compared to DVR, baseline SRTM BP_{SO} showed a small bias (≤ 6.1%) with lower precision for shorter acquisition times, while $SUVR_{SO,60\text{-}90min}$ showed 3.5% bias with similar precision. Differences between SV2A occupancy values based on $SUVR_{SO,60\text{-}90min}$ and occupancy estimates using V_T and a Lassen plot were small but significant, while negligible bias was found for SRTM based occupancy estimates (at least 70 min acquisition).

Conclusion This [^{11}C]UCB-J blocking study validated SO as a suitable reference region for non-invasive quantification of SV2A availability and drug occupancy in the human brain. Accurate quantification can be achieved by using either $SUVR_{SO,60\text{-}90min}$ with a 60–90 min PET acquisition or SRTM BP_{SO} with at least 70 min dynamic PET acquisition.

Keywords Positron emission tomography · Synaptic density · Reference tissue · Kinetic modelling · [^{11}C]UCB-J

Introduction

Synaptic vesicle glycoprotein 2A (SV2A) [1–3] is an integral membrane protein, located in the presynaptic vesicle membrane, ubiquitously and homogenously expressed in all synapses across the brain. Synaptic pathology is a fundamental finding in many post-mortem studies and has been associated with many neurological and psychiatric disorders. Reduced synaptic density has been reported in the seizure onset zone of patients with epilepsy [4–6]. Moreover, also in stroke, traumatic brain injury, and various forms of neurodegeneration synaptic density changes are associated with clinical deficiencies. For example, decreased synaptic density in the hippocampus and cerebral cortex is closely related with cognitive impairment in Alzheimer's disease [7, 8]. Also in psychiatric disorders, such as autism [9], depression [10] and schizophrenia [11, 12], changes in synaptic density are thought to play a role in the phenotyping of the disease.

Development of levetiracetam-based radioligands, such as [^{11}C]UCB-A [13], [^{18}F]UCB-H [14] and most recently also [^{11}C]UCB-J [3], expressing high affinity and specificity for

Electronic supplementary material The online version of this article (https://doi.org/10.1007/s00259-018-4119-8) contains supplementary material, which is available to authorized users.

✉ Michel Koole
michel.koole@kuleuven.be

[1] Department of Nuclear Medicine and Molecular Imaging, KU Leuven, Herestraat 49, 3000 Leuven, Belgium

[2] UCB Pharma, Braine-l'Alleud, Belgium

SV2A, enable in vivo positron emission tomography (PET) imaging of presynaptic SV2A expression. More specifically, [^{11}C]UCB-J has demonstrated optimal pharmacokinetics and quantification properties with no evidence of brain penetrating radiometabolites [2]. As such, the distribution volume of [^{11}C]UCB-J binding in brain tissue is considered to be an excellent in vivo proxy of synaptic density [2]. To further support research on synaptic pathology and improve clinical applicability, we propose and evaluate a minimally invasive, reference tissue based quantification of synaptic density in the human brain using [^{11}C]UCB-J PET imaging. For this purpose, we first determined whether the distribution volume of [^{11}C]UCB-J uptake in subcortical white matter (specifically the centrum semi-ovale) is representative for non-displaceable [^{11}C]UCB-J uptake in target brain regions using human blocking studies. Second, we compared the distribution volume ratio of [^{11}C]UCB-J brain uptake relative to the centrum semi-ovale determined by full kinetic modeling with reference tissue based estimates for specific over non-displaceable tracer binding using centrum semi-ovale as reference tissue. Third, we evaluated the time-stability of the kinetic parameters by reducing the acquisition time and evaluated a static reference tissue approach to analyze [^{11}C]UCB-J PET blocking studies and to determine the corresponding SV2A occupancy.

Materials and methods

Study design and [^{11}C]UCB-J PET/MR imaging

Dynamic PET data were acquired in the context of a PET dose occupancy study to evaluate receptor occupancy of padsevonil (UCB Pharma, Brussels, Belgium), an investigational new drug for epilepsy with a selective affinity for both presynaptic synaptic vesicle 2 (SV2) proteins and postsynaptic central benzodiazepine receptor (cBZR) sites on the gamma-aminobutyric acid ($GABA_A$) receptor. At presynaptic sites, padsevonil binds with high affinity to all three subtypes of the human synaptic vesicle 2 (hSV2) protein (ie, SV2A, SV2B, and SV2C). In total, ten carefully screened healthy volunteers (8 males and 2 females, age 27.6 ± 10.0 years (mean ± SD) with an age range of 20–54 years) underwent baseline scanning. Next, all subjects received a single oral dose of padsevonil ranging from 6.25 up to 100 mg. Post drug PET scanning was performed at 2 h (7 scans), 6 h (4 scans), 24 h (4 scans), 27 h (1 scan) and 30 h (2 scans) after drug administration. Dose range and timing of the post drug PET scans were based on the adaptive design of this study to achieve different plasma levels of the drug and therefore different exposure and occupancy levels in the brain. This way, an optimal sampling of the dose occupancy curve could be achieved. In total, 17 post dose PET scans were performed with two post drug PET scans performed for seven subjects and only one post dose PET scan performed for three subjects. The injected activity of [^{11}C]UCB-J was 232.6 ± 67.7 MBq (mean ± SD), with a specific activity of 91.3 ± 38.2 GBq/μmol and injected mass of 0.98 ± 0.63 μg. The study was approved by the Ethics Committee of the local University Hospital where the study took place. Informed consent was obtained from all individual participants included in the study.

Image acquisition and reconstruction parameters on the GE Signa PET/MR are given in the Supplementary Materials and Methods in detail. The synthesis, radiolabeling and quality control of [^{11}C]UCB-J was done according to the same procedure as described previously [3].

[^{11}C]UCB-J brain PET kinetic modeling

Regional total distribution volume estimates (V_T) were determined by applying a 1 and 2 tissue compartment model (1TCM – 2TCM) with fixed blood volume of 5% and using the composite cortical time activity curve (TAC) to estimate potential small time shifts between PET TAC and arterial blood/plasma input functions. The Akaike Information Criterion (AIC) and F-test were used to select the most appropriate model for V_T estimation. Next, V_T estimates using a non-compartment Logan Graphical Analysis (LGA) [15] were compared to V_T values estimated with the most appropriate kinetic model.

SV2A occupancy estimates using regional [^{11}C]UCB-J V_T values and a Lassen plot

With V_S^{base} and V_S^{drug} representing the regional distribution volumes for specific tracer binding before and after drug administration, respectively, the regional, drug-induced fractional target occupancy O_S can be estimated as the relative change in specific binding between baseline and post drug PET scanning:

$$O_S = \frac{V_S^{base} - V_S^{drug}}{V_S^{base}} \quad (1)$$

If only regional V_T values are available as quantitative endpoints as is the case for 1TCM based quantification, the Lassen plot [16] combines baseline and post drug PET scanning to determine a global, drug-induced occupancy level. Considering that $V_T = V_{ND} + V_S$ with V_{ND} the distribution volume for non-displaceable tracer binding and assuming that V_{ND} remains constant for baseline and post drug PET scanning, Eq. (1) can be rewritten as a Lassen plot:

$$V_T^{base} - V_T^{drug} = O_{Lassen}\left(V_T^{base} - V_{ND}\right) \quad (2)$$

with the slope O_{Lassen} representing a global, drug-induced occupancy estimate for all considered brain regions. Using this approach and a non-weighted least squares fitting, global

SV2A occupancy can be estimated based on regional [^{11}C]UCB-J V_T values determined with the most appropriate kinetic model. This global SV2A occupancy estimate O_{Lassen} was considered as reference value for further method comparison.

Validation of centrum semi-ovale as reference region for [^{11}C]UCB-J brain PET quantification

To consider the centrum semi-ovale as a suitable reference region for [^{11}C]UCB-J brain PET quantification, specific [^{11}C]UCB-J binding in this brain region should be negligible such that the administration of a SV2A specific drug does not induce significant changes in the centrum semi-ovale distribution volume V_{SO}. Therefore we compared baseline and post drug [^{11}C]UCB-J V_{SO} to evaluate potential drug-induced changes.

On the other hand, V_{SO} should be representative for V_{ND}. As such, regional V_S^{base} and V_S^{drug} values together with corresponding O_{SO} , can be estimated directly by subtracting V_{SO} from the regional V_T^{base} and V_T^{drug} values and using a non-weighted least squares fitting of Eq. (1). As the Lassen plot does not make any assumptions about a reference region, we compared O_{SO} with O_{Lassen} occupancy values to evaluate the validity of centrum semi-ovale as reference tissue for [^{11}C]UCB-J brain uptake.

Validation and time stability of simplified [^{11}C]UCB-J brain PET quantification using centrum semi-ovale as reference region

Once [^{11}C]UCB-J uptake in the centrum semi-ovale was established as representative for non-displaceable [^{11}C]UCB-J uptake in the brain, a Simplified Reference Tissue Model (SRTM2) using centrum semi-ovale as reference tissue was evaluated to quantify [^{11}C]UCB-J brain uptake. For this purpose, a global, constant reference region clearance constant k_2 was considered for all target brain regions. Moreover, regional SRTM2 $BP_{SO,\ 90}$ [17] values using the full 90 min dynamic PET data were compared with corresponding $V_T/V_{SO} - 1$ values, denoted as $DVR_{SO} - 1$.

Next, a reduction in acquisition time was evaluated by considering an acquisition time of 80 min, 70 min and 60 min starting at the time of tracer injection for SRTM2 BP_{SO} quantification ($BP_{SO,\ 80}$, $BP_{SO,\ 70}$ and $BP_{SO,\ 60}$ respectively). Finally, $DVR_{SO}$was estimated by a Standard Uptake Value Ratio (SUVR) relative to the centrum semi-ovale region. For this approach, equilibrium tracer binding data of a single static PET frame ($SUVR_{SO}$) were evaluated as a proxy for $DVR_{SO} - 1$. The appropriate starting point and frame duration for the $SUVR_{SO}$ estimation was based on the time stability of the cortical SUVR relative to the tracer uptake in the centrum semi-ovale region.

Considering that $BP_{SO} = DVR_{SO} - 1$ and V_{SO} remains constant for all brain regions and for baseline and post drug PET scanning, Eq. (1) corresponds to:

$$O_{BP} = \frac{BP_{SO}^{base} - BP_{SO}^{drug}}{BP_{SO}^{base}} \quad (3)$$

Based on this approach, O_{BP} occupancy values were calculated for SRTM2 $BP_{SO,\ 90}$, $BP_{SO,\ 80}$, $BP_{SO,\ 70}$ and $BP_{SO,\ 60}$ values by applying a non-weighted least squares fit. Similarly, O_{SUVR} were calculated by substituting BP_{SO}^{base} and BP_{SO}^{drug} with $SUVR_{SO}^{base} - 1$ and $SUVR_{SO}^{drug} - 1$ respectively. O_{BP} and O_{SUVR} occupancy values were compared with O_{Lassen} values determined with the Lassen plot (2) to further validate the SRTM2 approach with the centrum semi-ovale as reference region and to evaluate the impact of SUVR as model simplification.

Statistics

A two-way repeated measures analysis of variance (ANOVA) with Bonferroni posttests was used to evaluate the impact of different kinetic models on regional V_T values and to assess the regional occupancy effect. V_T based occupancy estimates using SO as reference tissue were compared with a Lassen plot using a Wilcoxon Signed Rank test and a Bland Altman analysis. Once the appropriate kinetic model and reference tissue were validated, a Spearman correlation and linear regression analysis (forced through the origin) was performed for all conditions and for baseline and post drug conditions separately, to evaluate the relationship between $DVR_{SO} - 1$ and BP_{SO} using different reference tissue models. For baseline conditions only, a Bland Altman analysis and two-way repeated measures ANOVA with Bonferroni posttests evaluated the impact of different reference tissue approaches on regional, baseline BP_{SO} values. BP_{SO} based occupancy estimates were compared with a one-way ANOVA (Friedman test with Dunn's multiple comparisons) and Bland Altman analysis to evaluate the agreement between different reference tissue models for different acquisition time intervals.

Results

Full kinetic modeling of [^{11}C]UCB-J

Regional 1TCM, 2TCM and LGA V_T values for [^{11}C]UCB-J at baseline are presented in Table 1. Representative LGA V_T parametric maps for a baseline [^{11}C]UCB-J PET scan and a post drug [^{11}C]UCB-J PET scan taken 2 h after single dosing

Table 1 1- and 2-Tissue Compartment Model (1-2TCM) V_T values together with Logan graphical analysis (LGA) V_T for baseline PET scanning ($n = 10$). Data are presented as mean ± SD

Region	1TCM	2TCM	LGA
Composite cortex	30.0 ± 4.0	30.2 ± 4.5	29.5 ± 4.6
Frontal cortex	29.6 ± 3.8	29.9 ± 4.2	29.2 ± 4.3
Temporal cortex	30.1 ± 4.2	30.4 ± 4.7	29.5 ± 4.7
Parietal cortex	30.9 ± 4.2	31.2 ± 4.7	30.5 ± 4.8
Occipital cortex	29.4 ± 4.2	29.6 ± 4.6	28.9 ± 4.7
Insula	31.4 ± 4.7	31.7 ± 5.2	30.8 ± 5.2
Anterior cingulum	32.0 ± 4.3	32.3 ± 4.7	31.5 ± 4.8
Posterior cingulum	33.9 ± 3.9	34.2 ± 4.3	33.5 ± 4.3
Striatum	32.0 ± 4.6	32.2 ± 4.9	31.2 ± 5.0
Thalamus	25.1 ± 2.3	25.3 ± 2.5	24.7 ± 2.5
Hippocampus	25.5 ± 4.5	25.9 ± 5.1	24.7 ± 4.6
Amygdala	29.5 ± 4.5	29.8 ± 5.1	28.1 ± 4.5
Cerebellum	22.7 ± 2.9	23.0 ± 3.4	22.6 ± 3.3
Brainstem	10.5 ± 1.3	10.7 ± 1.4	10.5 ± 1.4
Centrum semi-ovale	5.3 ± 0.6	5.3 ± 0.6	5.2 ± 0.6

with 6.25 mg of padsevonil and corresponding to a 57% occupancy level are shown in the supplementary Figure 1s.

1TCM AIC values were lower than 2TCM AIC values in 260 out of 405 VOI fits (cases) (64.2%) while the F-test indicated no significantly improved fittings ($p > 0.05$) for 2TCM compared to 1TCM in 267 out of 405 cases (65.9%). These findings suggested that 1TCM the is most suitable model for [^{11}C]UCB-J. A higher ratio of lower 1TCM AIC values compared to 2TCM AIC values was observed for baseline conditions (112 out of 150 cases; 74.7%), compared to post drug conditions (148 out of 255 cases; 58.0%) with a ratio of 40.7% (61 out of 150 cases) for the first post drug scan and a ratio of 82.9% (87 out of 105 cases) for the second post drug scan. This was confirmed by the F-test which presented no significantly better fittings ($p > 0.05$) for 2TCM compared to 1TCM in 121 out of 150 baseline cases (80.7%) and in 146 out of 255 post drug cases (57.3%) with a ratio of 40.7% (61 out of 150 cases) for the first post drug scan and a ratio of 81.0% (85 out of 105 cases) for the second post drug scan. Furthermore, both AIC and F-test determined 1TCM as the preferred model for centrum semi-ovale tracer kinetics in 26 out of 27 fittings (96.3%). As 1TCM was found to be the preferred compartmental model, a detailed overview of regional 1TCM K_1 and k_2 values for baseline and post drug [^{11}C]UCB-J PET scanning is given in the supplementary Table 1s.

For regional [^{11}C]UCB-J V_T values, a two-way repeated measures analysis of variance (ANOVA) showed a significant interaction between brain region and kinetic model ($p < 0.0001$), but Bonferroni posttests revealed no significant differences between 1TCM and 2TCM V_T values for all brain regions. However, LGA V_T were significantly lower ($p < 0.05$) compared to 1TCM V_T values for all brain regions except for the occipital cortex, cerebellum, brainstem and centrum semi-ovale.

Validation of centrum semi-ovale as a reference region for [^{11}C]UCB-J brain PET quantification

As 1TCM proved to be the preferred compartmental model to describe [^{11}C]UCB-J tracer kinetics in the brain, 1TCM V_T values of baseline and post drug PET scanning were further analyzed using a two-way repeated measures ANOVA to determine the regional occupancy effect. This was done in two different designs. A first design included all ten subjects with their respective baseline and first PET post drug scan, while a second design included seven subjects with their respective baseline and two post drug scans. Both analyses showed a significant interaction between brain region and dosing ($p < 0.0001$), while Bonferroni posttests for the first design demonstrated a significant difference in V_T values between baseline and the first post drug PET scan for all brain regions ($p < 0.001$) except for the centrum semi-ovale ($p > 0.05$). Bonferroni posttests for the second design confirmed these results ($p < 0.05$) except for the brainstem. For this region, differences in V_T values between baseline and the second post drug PET scan were not significant ($p > 0.05$). For the centrum semi-ovale, post drug 1TCM V_{SO} values were 4.9 ± 0.9 (mean ± SD) compared to baseline 1TCM V_{SO} values of 5.3 ± 0.6 (see Table 1). A graphical overview of the individual baseline and post drug 1TCM V_{SO} is given in the supplementary Figure 2s.

1TCM V_T values using a Lassen plot gave overall occupancy estimates of 65.3 ± 26.8% (mean ± SD) with a 16–98% range. For the first post drug scans, occupancy estimates were 82.1 ± 14.5% with a range of 57–98%, while for the second post drug scans, occupancy values were 41.2 ± 21.2% with a 16–63% range.

Cortical and centrum semi-ovale TACs of baseline and post drug scans of five different subjects corresponding to occupancy levels of 61.1 ± 2.9% are presented in Fig. 1a with corresponding baseline and post drug 1TCM, 2TCM and LGA V_T estimates presented in Fig. 2. As such, mean baseline and post drug V_T can be assessed visually for a similar occupancy level, demonstrating limited inter-subject variability and substantial blocking for all brain regions except for the centrum semi-ovale. More specifically, Fig. 2 allows a visual assessment of the validity of centrum semi-ovale as reference region, since subtracting V_{SO} from other regional V_T values should result in the distribution volume of specific binding V_S for these brain regions. Consequently, differences between regional baseline and post drug V_S values should match an approximate 60% reduction in specific binding corresponding to a small range of occupancy levels around 60%, represented by these datasets.

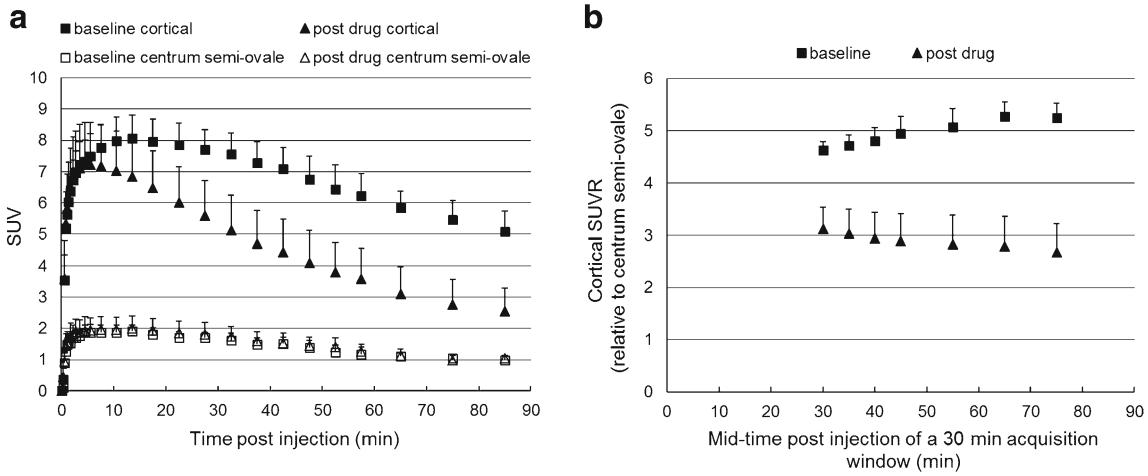

Fig. 1 Baseline and post drug cortical and centrum semi-ovale TACs of five different subjects representing a mean occupancy level of 61.1 ± 2.9% (mean ± SD) (**a**) together with the corresponding cortical SUVR relative to the centrum semi-ovale for a 30 min PET frame at different time points post tracer injection (**b**)

In terms of occupancy estimates, no significant difference was found between O_{SO} and O_{Lassen} values (Wilcoxon Signed Rank Test, $p > 0.05$). A Bland Altman comparison with 1TCM O_{Lassen} data (% difference vs average, see Fig. 3) showed a mean 1.9% bias with 2.8% SD and [−3.7%, 7.5%] as the 95% limits of agreement interval.

Validation and time stability of simplified [^{11}C]UCB-J brain PET quantification using centrum semi-ovale as reference region

Representative $SUVR_{SO,\ 60-90} - 1$ and SRTM2 $BP_{SO,\ 90}$ parametric maps for a baseline and post drug [^{11}C]UCB-J PET scan are shown in the supplementary Figure 1s. A Spearman correlation and linear regression analysis (forced through the origin) was performed between 1TCM $DVR_{SO} - 1$ on the one hand and $SUVR_{SO,\ 60-90} - 1$, SRTM2 $BP_{SO,\ 90}$, SRTM2 $BP_{SO,\ 80}$, SRTM2 $BP_{SO,\ 70}$ and SRTM2 $BP_{SO,\ 60}$ on the other hand to evaluate the relationship between the different approaches (see Table 2) for all conditions and for baseline and post drug conditions separately. For the $SUVR_{SO}$ approach, a single 30 min PET frame starting at 60 min post injection ($SUVR_{SO,\ 60-90}$) was considered based on the time stability of the cortical SUVR relative to the tracer uptake in the centrum semi-ovale as presented in Fig. 1b. Results revealed highly significant correlations ($p < 0.0001$) between 1TCM $DVR_{SO} - 1$ and $SUVR_{SO,\ 60-90} - 1$, SRTM2 $BP_{SO,\ 90}$, SRTM2 $BP_{SO,\ 80}$, SRTM2 $BP_{SO,\ 70}$ and SRTM2 $BP_{SO,\ 60}$ respectively, with a slightly lower correlation value for SRTM2 $BP_{SO,\ 60}$ at baseline. In terms of linear regression analysis, slope values, indicative for bias, were similar for

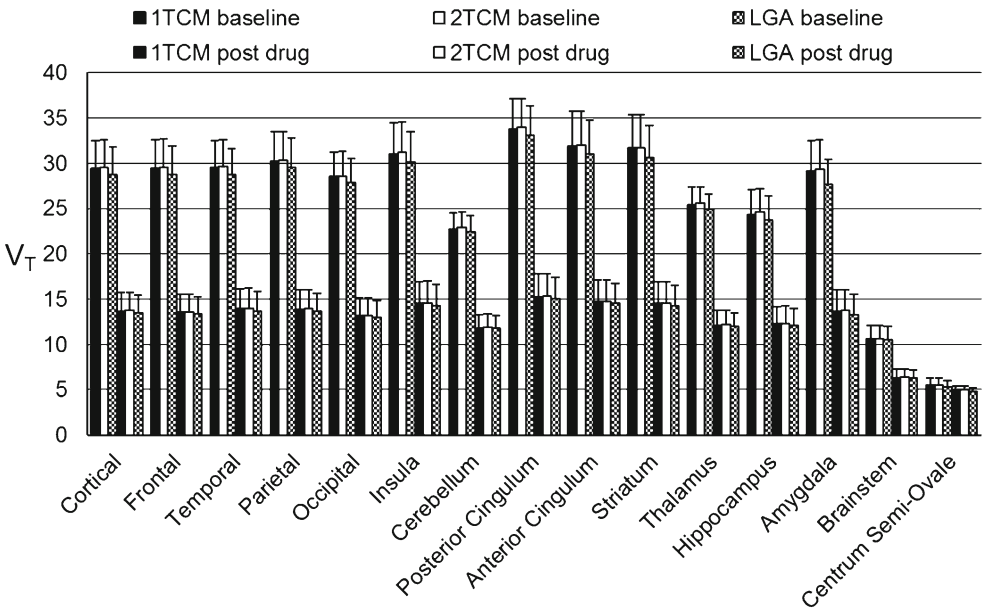

Fig. 2 Mean baseline and post drug 1TCM, 2TCM and LGA $V_T$values (SD as error bar) for five different subjects corresponding to a mean occupancy level of 61.1 ± 2.9% (mean ± SD). The higher range of $V_T$values corresponds to baseline while the lower range corresponds to post treatment conditions

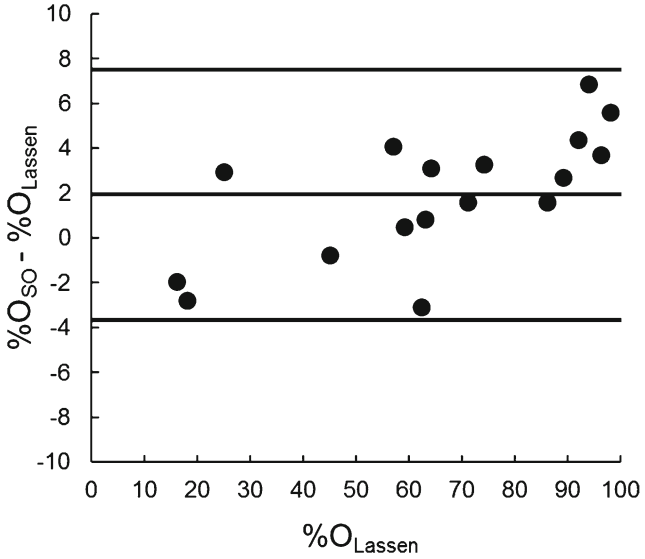

Fig. 3 A Bland Altman comparison between SO based occupancy estimates O_{SO} and 1TCM V_T based occupancy estimates O_{Lassen} resulting in a 1.9% bias with 2.8% SD and [−3.7%, 7.5%] as the 95% limits of agreement

all approaches and consistent for baseline and post drug scanning. On the other hand, goodness of fit values, representing the root mean square error, increased for baseline scanning compared to post dose scanning with higher values for shorter acquisition times, indicating a less optimal straight line fit for these SRTM2 approaches. These findings were confirmed by visual assessment of the scatter plots for the composite cortical region as presented in Fig. 4 for both baseline and post drug conditions, demonstrating a less optimal straight line fit for baseline conditions.

Baseline regional 1TCM $DVR_{SO} - 1$, $SUVR_{SO,\ 60-90} - 1$, SRTM2 $BP_{SO,\ 90}$, SRTM2 $BP_{SO,\ 80}$, SRTM2 $BP_{SO,\ 70}$ and SRTM2 $BP_{SO,\ 60}$ values for [^{11}C]UCB-J brain uptake are presented in Table 3. A two-way repeated measures ANOVA showed no significant interaction between brain regions and the different approaches to estimate baseline BP_{SO} using the centrum semi-ovale as reference tissue. Moreover, Bonferroni posttests revealed no significant differences between baseline 1TCM $DVR_{SO} - 1$, SRTM2 $BP_{SO,\ 80}$, and SRTM2 $BP_{SO,\ 70}$ values for all brain regions, while differences between baseline 1TCM $DVR_{SO} - 1$ and SRTM2 $BP_{SO,\ 90}$ and between baseline 1TCM $DVR_{SO} - 1$ and SRTM2 $BP_{SO,\ 60}$ values were only significant for temporal cortex and amygdala and for temporal cortex, hippocampus and amygdala, respectively. Additionally, no significant differences between baseline 1TCM $DVR_{SO} - 1$ and $SUVR_{SO,\ 60-90} - 1$ values were found except for the amygdala.

Again for baseline conditions, a Bland Altman analysis (% difference vs average) comparing $SUVR_{SO,\ 60-90} - 1$, SRTM2 $BP_{SO,\ 90}$, SRTM2 $BP_{SO,\ 80}$, SRTM2 $BP_{SO,\ 70}$ and SRTM2 $BP_{SO,\ 60}$ with 1TCM $DVR_{SO} - 1$, revealed a negative bias for all approaches in line with the slope of the linear regression (see Table 2, Table 4 and corresponding plots in supplementary Figure 3s). For the SRTM2 approach, the standard deviation of the bias and the corresponding 95% limits of agreement interval increased as the acquisition time was shortened. These findings were also in line with the goodness of fit values of the linear regression analysis and were confirmed by a box plot of the ratio of baseline SRTM2 $BP_{SO,\ x}$ (with x = 60, 70, 80, or 90 min) and $SUVR_{SO,\ 60-90} - 1$ values relative to baseline 1TCM $DVR_{SO} - 1$ values as presented in Fig. 5. This plot again demonstrated a very limited, insignificant bias for all approaches. Variability for SRTM2 BP_{SO} estimates increased however with shorter acquisition times.

In terms of occupancy, a statistically significant difference was found between O_{Lassen}, O_{SUVR} and O_{BP} occupancy values for different acquisition time intervals as determined by one-way ANOVA (Friedman test, $p < 0.05$). Dunn's multiple comparison posttests revealed significantly higher O_{SUVR} occupancy values ($p < 0.05$) compared to O_{Lassen} values.

A Bland Altman comparison (%difference vs average) of O_{SUVR} and O_{BP} occupancy values for the different acquisition

Table 2 Spearman correlation and linear regression analysis (straight line through the origin) between 1TCM $DVR_{SO} - 1$ values and $SUVR_{SO,\ 60-90} - 1$, SRTM2 $BP_{SO,\ 90}$, SRTM2 $BP_{SO,\ 80}$, SRTM2 $BP_{SO,\ 70}$ and SRTM2 $BP_{SO,\ 60}$ values. All approaches use the centrum semi-ovale (SO) as reference tissue. All correlations are highly significant ($p < 0.001$)

Measure	$SUVR_{SO}$-1 (60-90 min)	SRTM2 BP_{SO}90 min	SRTM2 BP_{SO}80 min	SRTM2 BP_{SO}70 min	SRTM2 BP_{SO}60 min
Baseline & post drug ($N = 27$)					
Spearman rho	0.99	1.00	1.00	0.99	0.99
Slope	0.96	0.95	0.97	0.97	0.94
Goodness of fit (Sy.x)	0.21	0.12	0.15	0.22	0.30
Baseline (N = 10)					
Spearman rho	0.94	0.98	0.96	0.95	0.89
Slope	0.97	0.95	0.96	0.97	0.94
Goodness of fit (Sy.x)	0.24	0.14	0.21	0.32	0.43
Post drug ($N = 17$)					
Spearman rho	0.99	1.00	1.00	0.99	0.98
Slope	0.94	0.97	0.98	0.96	0.94
Goodness of fit (Sy.x)	0.18	0.09	0.10	0.20	0.22

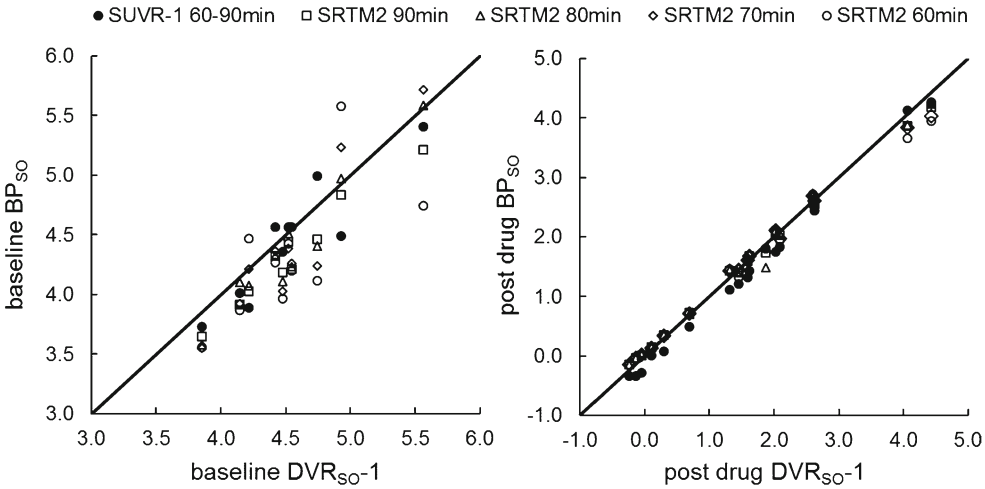

Fig. 4 Scatter plots for the composite cortical region of SRTM2 $BP_{SO,\ x}$ values for the different acquisition time intervals vs 1TCM $DVR_{SO} - 1$ values for both baseline and post drug conditions

time intervals with O_{Lassen} occupancy values are presented in Table 5 with the corresponding plots presented in supplementary Figure 4s. Results demonstrated a small bias and 95% limits of agreement interval of around ±12% for SRTM2 $BP_{SO,\ 90}$, SRTM2 $BP_{SO,\ 80}$ and SRTM2 $BP_{SO,\ 70}$. On the other hand, $SUVR_{SO,\ 60-90} - 1$ occupancy values showed a slightly higher bias with a similar 95% limits of agreement interval while SRTM2 $BP_{SO,\ 60}$ demonstrated both a higher bias and a twice as large 95% limits of agreement interval.

Discussion

Full kinetic modeling using both AIC and F-test criteria confirmed 1TCM as the preferred model for [^{11}C]UCB-J brain PET quantification [18]. Our AIC and F-test results were consistent and in line with previous studies comparing different model selection criteria and stating that both AIC and F-test are effective and efficient approaches, resulting in similar conclusions [19–21]. However, the most suitable model to describe [^{11}C]UCB-J tracer kinetics depended on the degree of SV2A occupancy. Whereas 1TCM was clearly the most appropriate kinetic model for the baseline and second post drug [^{11}C]UCB-J PET scans, 2TCM was the preferred model to describe [^{11}C]UCB-J tracer kinetics for the first post dose PET scans which represented the highest range of SV2A occupancy. This is in line with previous findings for preclinical [^{11}C]Flumazenil brain PET scanning where 2TCM was suggested as the preferred kinetic model [22] but for regions with high levels of specific binding, the contribution of the non-specific component to the overall signal became too small to distinguish two kinetically different compartments and 1TCM

Table 3 Baseline BP_{SO} values calculated as DVR–1, SUVR–1 for a 60 to 90 min acquisition post injection and using SRTM2 for a 90, 80, 70 and 60 min scan starting at tracer injection. For all approaches, centrum semi-ovale (SO) is used as reference tissue. Data are presented as mean ± SD

Region	1TCM DVR_{SO}-1 (90 min)	$SUVR_{SO}$-1 (60-90 min)	SRTM2 BP_{SO} 90 min	SRTM2 BP_{SO} 80 min	SRTM2 BP_{SO} 70 min	SRTM2 BP_{SO} 60 min
Composite cortex	4.54 ± 0.47	4.46 ± 0.50	4.33 ± 0.45	4.39 ± 0.55	4.39 ± 0.63	4.32 ± 0.55
Frontal cortex	4.47 ± 0.43	4.41 ± 0.51	4.30 ± 0.41	4.36 ± 0.49	4.36 ± 0.54	4.31 ± 0.48
Temporal cortex	4.56 ± 0.56	4.36 ± 0.53	4.24 ± 0.55	4.32 ± 0.68	4.32 ± 0.81	4.21 ± 0.71
Parietal cortex	4.76 ± 0.46	4.68 ± 0.50	4.54 ± 0.43	4.60 ± 0.53	4.60 ± 0.61	4.53 ± 0.51
Occipital cortex	4.44 ± 0.54	4.36 ± 0.54	4.26 ± 0.50	4.32 ± 0.62	4.34 ± 0.71	4.27 ± 0.61
Insula	4.81 ± 0.57	4.63 ± 0.54	4.50 ± 0.55	4.58 ± 0.69	4.60 ± 0.81	4.50 ± 0.68
Posterior cingulum	5.24 ± 0.60	5.18 ± 0.62	5.01 ± 0.56	5.06 ± 0.61	5.05 ± 0.67	5.00 ± 0.68
Anterior cingulum	4.87 ± 0.59	4.73 ± 0.63	4.56 ± 0.59	4.64 ± 0.71	4.64 ± 0.81	4.57 ± 0.78
Striatum	4.91 ± 0.55	4.77 ± 0.52	4.74 ± 0.56	4.84 ± 0.72	4.87 ± 0.84	4.79 ± 0.69
Thalamus	3.65 ± 0.36	3.61 ± 0.39	3.54 ± 0.32	3.55 ± 0.29	3.54 ± 0.31	3.51 ± 0.31
Hippocampus	3.72 ± 0.60	3.51 ± 0.47	3.40 ± 0.53	3.46 ± 0.67	3.48 ± 0.80	3.34 ± 0.49
Amygdala	4.45 ± 0.57	3.96 ± 0.43	4.02 ± 0.59	4.15 ± 0.83	4.21 ± 1.09	4.05 ± 0.89
Cerebellum	3.17 ± 0.39	3.18 ± 0.42	3.06 ± 0.32	3.06 ± 0.34	3.04 ± 0.34	2.99 ± 0.26
Brainstem	0.93 ± 0.15	0.82 ± 0.15	0.97 ± 0.16	0.95 ± 0.16	0.95 ± 0.16	0.96 ± 0.15

Table 4 Bland Altman comparison of baseline SUVR-1 for a 60 to 90 min acquisition after tracer injection and baseline SRTM2 BP_{SO} values for a 90, 80, 70 and 60 min acquisition starting at tracer injection with baseline 1TCM DVR-1 (%difference vs average). All approaches use the centrum semi-ovale (SO) as reference brain tissue

Measure	$SUVR_{SO}$-1 (60-90 min)	SRTM2 BP_{SO} 90 min	SRTM2 BP_{SO} 80 min	SRTM2 BP_{SO} 70 min	SRTM2 BP_{SO} 60 min
Bias (%)	−3.2	−5.5	−4.3	−4.4	−6.1
SD of bias (%)	5.5	3.6	5.0	7.1	9.6
95% limits of agreement (%)	[−14.0,7.7]	[−12.6,1.5]	[−14.0,5.4]	[−18.4,9.5]	[−24.9,12.7]

became more appropriate to describe tracer kinetics. However, no significant differences were found between [^{11}C]UCB-J 1TCM and 2TCM V_T values. Furthermore, for most clinical applications of [^{11}C]UCB-J brain PET imaging where changes between pathologies versus normal conditions are investigated, a lower reduction in specific binding is expected compared to the occupancy range of the first post PET scans. Therefore, 1TCM can be considered as the reference kinetic model for [^{11}C]UCB-J brain PET quantification for future clinical applications. Although differences were limited, LGA V_T values were significantly lower than 1TCM V_T values, in line with literature data which report an underestimation of V_T by a Logan plot [23].

Subcortical white matter has already been suggested as a reference region for [^{11}C]UCB-J brain PET quantification based on self-blocking studies in rhesus monkeys [3]. Therefore, we considered both a SUVR and reference tissue approach using centrum semi-ovale as reference region for quantification of [^{11}C]UCB-J PET imaging of the human brain. For the centrum semi-ovale as candidate reference region, we found no significant differences in this study between baseline and post dose 1TCM V_{SO} values, indicating negligible specific binding and thus target expression in this brain region. Furthermore, occupancy values estimated with V_{SO} as measure for the non-displaceable binding showed only limited bias with very good precision. We also considered comparing V_{ND} estimates of the Lassen plot with 1TCM V_{SO} values to further validate the centrum semi-ovale as reference tissue. However, the standard error for the V_{ND} estimates of the Lassen plot indicated the limited precision of these estimates, resulting in an average value of 4.67 ± 2.29 (mean ± SD) with a range from 2.74 to 10.78 and a coefficient of variation (COV) of 49%. On the other hand, 1TCM V_{SO} estimates represented an average value of 4.99 ± 0.79 with a range from 3.77 to 7.70 and COV of 16%.

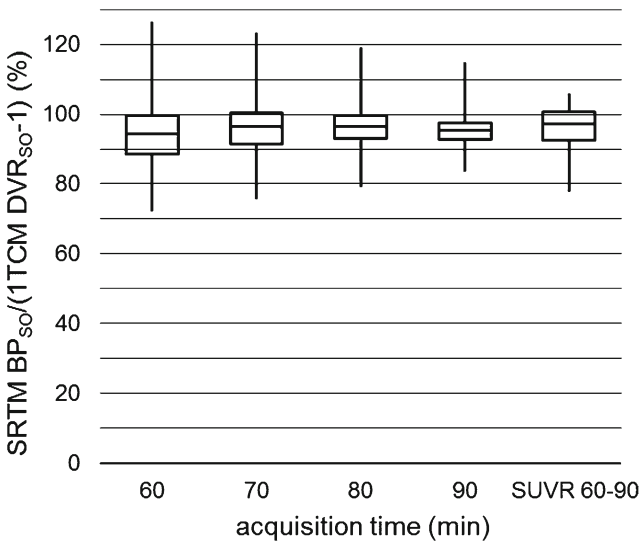

Fig. 5 A box plot of the ratio of baseline SRTM2 $BP_{SO,\,x}$ and $SUVR_{SO,\,60-90} - 1$ values relative to baseline 1TCM $DVR_{SO} - 1$ values for the different acquisition time intervals, demonstrating very limited bias for all acquisition time intervals with an increasing variability of SRTM2 $BP_{SO,\,x}$ for shorter acquisition time intervals

1TCM was consistently the model of preference for describing [^{11}C]UCB-J tracer kinetics in the centrum semi-ovale, both for baseline and post dose scanning with no impact of drug dosing. On the other hand, one would expect 2TCM to be the preferred model for centrum semi-ovale tracer kinetics since 2TCM was the most appropriate kinetic model for the first post drug scanning sessions corresponding with lowest levels of specific tracer binding. Although this could indicate differences in tracer kinetics between the centrum semi-ovale and target grey matter brain regions, findings of this study demonstrate the appropriate use of subcortical white matter as reference region for the quantification of [^{11}C]UCB-J binding in the human brain.

Since 1TCM is a suitable model for tracer kinetics of both the candidate reference region and target brain regions, a Simplified Reference Tissue Model (SRTM) was considered as the most appropriate reference tissue modeling approach. For this SRTM [17] approach, we coupled the efflux rate constant from the reference tissue back to the plasma for all brain regions to give a global, more robust estimate (SRTM2). Other reference tissue approaches, such as a multilinear or Logan reference tissue models, were not considered for this VOI based validation, especially since the latter requires population [24] based foreknowledge about the efflux rate constant between reference tissue and plasma.

Regarding time-stability, we compared SRTM2 BP_{SO} using centrum semi-ovale as reference region and 60, 70, 80 and 90 min dynamic PET data with 1TCM $DVR_{SO} - 1$ values. Referring to Table 3, baseline BP_{SO} are very similar for the

Table 5 Bland Altman comparison of occupancy values based on SUVR-1 for a 60 to 90 min acquisition after tracer injection and SRTM2 BP_{SO} for a 90, 80, 70 and 60 min acquisition time interval starting at tracer injection with 1TCM V_T occupancy values using a Lassen plot (%difference vs average). All but the latter approach use the centrum semi-ovale (SO) as reference tissue

Measure	$SUVR_{SO}$-1 (60-90 min)	SRTM2 BP_{SO} 90 min	SRTM2 BP_{SO} 80 min	SRTM2 BP_{SO} 70 min	SRTM2 BP_{SO} 60 min
Bias (%)	3.5	−1.2	−0.6	−0.6	3.7
SD of bias (%)	6.5	5.3	5.9	6.3	13.0
95% limits of agreement (%)	[−9.7,15.6]	[−11.6,9.2]	[−12.2,11.0]	[−13.0,11.8]	[−21.8,29.3]

different approaches with cortical BP_{SO} of 4.33 ± 0.45 (mean ± SD, CoV = 10.4%) for a 90 min acquisition time interval. We only reported baseline BP_{SO} values explicitly since these are clinically the most relevant and tracer kinetics of the post drug PET scans are faster and therefore less critical for a reduction of the acquisition time. This was demonstrated by the linear regression analysis showing that the goodness of fit to a straight line is decreased for baseline scanning compared to post dose scanning especially for shorter acquisition times (see Table 2 and Fig. 4). A Bland Altman analysis comparing baseline SRTM2 BP_{SO} values for different acquisition times with baseline 1TCM $DVR_{SO} - 1$ values (Table 4) revealed a negative bias of −5.5% with 95% limits of agreement of [−12.6%,1.5%] for a 90 min acquisition time. For shorter acquisition times, precision of the SRTM2 approach is lower, while the impact on the bias is limited. This is substantiated by the box plot in Fig. 5. A Bland Altman analysis comparing SRTM2 based occupancy estimates for different acquisition times with 1TCM based occupancy estimated using a Lassen plot, showed a small negative bias of −1.2% with 95% limits of agreement of [−11.6%,9.2%] for a 90 min acquisition time. Furthermore, an acquisition time of at least 70 min is required to obtain comparable bias and precision while an acquisition time of 60 min induced both a higher bias and twice as large 95% limits of agreement interval for SRTM2 based occupancies. These findings are supported by a 2-way repeated measures ANOVA comparing baseline 1TCM $DVR_{SO} - 1$ values with SRTM2 BP_{SO} values for different acquisition times and revealing significant differences between SRTM2 $BP_{SO,\ 90}$ and $BP_{SO,\ 60}$ values, with a higher number of regions for SRTM2 $BP_{SO,\ 60}$ compared to SRTM $BP_{SO,\ 90}$.

Since the precision of SRTM2 based occupancy estimates decreases substantially when the acquisition time is limited to 60 min, we considered SUVR relative to centrum semi-ovale for a 30 min acquisition time interval starting at 60 min after tracer injection. Although posttests of a 2-way repeated measures ANOVA revealed some significant differences between 1TCM $DVR_{SO} - 1$ and $SUVR_{SO,\ 60-90} - 1$ for most brain regions, correlations between both approaches remain very high (see Table 2). A Bland Altman analysis comparing 1TCM $DVR_{SO} - 1$ and $SUVR_{SO,\ 60-90} - 1$ yielded a negative bias of −3.2% with 95% limits of agreement of [−14.0%,7.7%] while comparing 1TCM based occupancy estimates with SUVR based values revealed a positive bias of 3.5% with [−9.7%,15.6%] as 95% limits of agreement. As such, a SUVR approach relative to the centrum semi-ovale presents itself as a valuable alternative for [^{11}C]UCB-J brain PET quantification instead of a more invasive, full kinetic modeling approach or an SRTM based approach, especially since the latter requires an acquisition time of at least 70 min. For instance, for studying synaptic pathology in specific patients groups such as cognitive impaired patients or patients with stroke and movement disorders, a SUVR approach could be preferred. Conversely, an SRTM approach also provides relative perfusion maps or R1 maps although it still needs to be determined if mapping the tracer delivery rate to target brain tissue relative to white matter comprises valuable information. Moreover, if an integrated PET/MR system is available, a static 30 min [^{11}C]UCB-J PET scan starting at 60 min after tracer injection can be combined with MR perfusion imaging to provide perfusion maps independent of a reference tissue and thus taking full advantage of simultaneous PET/MR.

Considering the limitations of this study, no test-retest variability data was available so far for the SRTM and SUVR based quantification approaches. A mean absolute test-retest reproducibility of 3–9% across brain regions was reported for [^{11}C]UCB-J V_T values [18, 25]. Since a non-invasive reference tissue approach obviates the need for tedious and logistically challenging arterial blood sampling, a full image based quantification approach will generally not increase test-retest variability. However, limited count statistics in the reference region due to lower tracer uptake or restricted size can have a negative impact on test-retest variability of BP_{ND} and SUVR estimates. Furthermore, this study only validated centrum semi-ovale as a reference region for [^{11}C]UCB-J brain PET quantification in young, healthy controls. It should preferably be reevaluated as a reference region for [^{11}C]UCB-J in patient groups, especially if pathological white matter involvement is expected (e.g. in neuro-inflammatory disorders). For this purpose, specific MR sequences can be considered to evaluate white matter integrity and exclude voxels for which white matter integrity can be questioned. To ensure a sufficiently large white matter reference region in terms of count statistics, one could include white matter voxels which are susceptible to spillover effects of (sub)cortical tracer uptake and which have been excluded for the current analysis. However, with a

proper and validated partial volume correction method, these voxels could be considered to improve the noise properties of the white matter PET signal.

Conclusion

Full kinetic modeling using arterial blood sampling confirmed 1TCM as the most suitable model for [^{11}C]UCB-J brain PET quantification. Dynamic PET imaging under baseline and pre-treatment conditions with a novel chemical entity with selective affinity for presynaptic SV2A, identified the centrum semi-ovale as a suitable reference region for [^{11}C]UCB-J brain PET quantification. Compared to a full kinetic analysis, a SRTM approach using a 90 min acquisition interval and the centrum semi-ovale as reference tissue shows a negligible bias and a bias of less than 6% for SV2A occupancy and density estimates respectively, both with acceptable precision. In terms of shortening the acquisition time, a dynamic acquisition of at least 70 min is needed to insure comparable bias and precision. A SUV ratio relative to the centrum semi-ovale for a 30 min acquisition starting 60 min after tracer injection provides similar bias and precision for both SV2A density and occupancy and can be considered as a valid quantitative proxy for simplified and clinically useful [^{11}C]UCB-J brain PET imaging.

Acknowledgments We thank Kwinten Porters and Jef Van Loock for their technical assistance, and the radiopharmacy team for the tracer productions. Part of this study was sponsored by a research grant of UCB to KU Leuven (principal investigator Koen Van Laere).

Compliance with ethical standards

Conflict of interest Brigitte Lacroix, Joel Mercier, David Sciberras and Paul Maguire are employees of UCB Pharma. Michel Koole, June van Aalst, Martijn Devrome, Nathalie Mertens, Kim Serdons and Koen Van Laere have no conflicts to disclose.

Ethical approval All procedures performed in studies involving human participants were in accordance with the ethical standards of the institutional and/or national research committee and with the 1964 Helsinki declaration and its later amendments or comparable ethical standards.

References

1. Bajjalieh SM, Frantz GD, Weimann JM, McConnell SK, Scheller RH. Differential expression of synaptic vesicle protein 2 (SV2) isoforms. J Neurosci. 1994;14:5223–35.
2. Finnema SJ, Nabulsi NB, Eid T, Detyniecki K, Lin SF, Chen MK, et al. Imaging synaptic density in the living human brain. Sci Transl Med. 2016;8:348ra96. https://doi.org/10.1126/scitranslmed.aaf6667.
3. Nabulsi NB, Mercier J, Holden D, Carre S, Najafzadeh S, Vandergeten MC, et al. Synthesis and preclinical evaluation of [^{11}C]UCB-J as a PET tracer for imaging the synaptic vesicle glycoprotein 2A in the brain. J Nucl Med. 2016;57:777–84. https://doi.org/10.2967/jnumed.115.168179.
4. Crevecoeur J, Kaminski RM, Rogister B, Foerch P, Vandenplas C, Neveux M, et al. Expression pattern of synaptic vesicle protein 2 (SV2) isoforms in patients with temporal lobe epilepsy and hippocampal sclerosis. Neuropathol Appl Neurobiol. 2014;40:191–204. https://doi.org/10.1111/nan.12054.
5. Feng G, Xiao F, Lu Y, Huang Z, Yuan J, Xiao Z, et al. Down-regulation synaptic vesicle protein 2A in the anterior temporal neocortex of patients with intractable epilepsy. J Mol Neurosci. 2009;39:354–9. https://doi.org/10.1007/s12031-009-9288-2.
6. Proper EA, Oestreicher AB, Jansen GH, Veelen CW, van Rijen PC, Gispen WH, et al. Immunohistochemical characterization of mossy fibre sprouting in the hippocampus of patients with pharmaco-resistant temporal lobe epilepsy. Brain J Neurol. 2000;123(Pt 1):19–30.
7. DeKosky ST, Scheff SW. Synapse loss in frontal cortex biopsies in Alzheimer's disease: correlation with cognitive severity. Ann Neurol. 1990;27:457–64. https://doi.org/10.1002/ana.410270502.
8. Hamos JE, DeGennaro LJ, Drachman DA. Synaptic loss in Alzheimer's disease and other dementias. Neurology. 1989;39:355–61.
9. Tang G, Gudsnuk K, Kuo SH, Cotrina ML, Rosoklija G, Sosunov A, et al. Loss of mTOR-dependent macroautophagy causes autistic-like synaptic pruning deficits. Neuron. 2014;83:1131–43. https://doi.org/10.1016/j.neuron.2014.07.040.
10. Kang H, Voleti B, Hajszan T, Rajkowska G, Stockmeier C, Licznerski P, et al. Decreased expression of synapse-related genes and loss of synapses in major depressive disorder. Nat Med. 2012;18:1413–7. https://doi.org/10.1038/nm.2886.
11. Glantz LA, Lewis DA. Decreased dendritic spine density on prefrontal cortical pyramidal neurons in schizophrenia. Arch Gen Psychiatry. 2000;57:65–73.
12. Sekar A, Bialas AR, de Rivera H, Davis A, Hammond TR, Kamitaki N, et al. Schizophrenia risk from complex variation of complement component 4. Nature. 2016;530:177–83. https://doi.org/10.1038/nature16549.
13. Lubberink M, Appel L, Daging J, Lindskog K, Danfors T, Larsson E-M, et al. Tracer kinetic analysis of the SV2A ligand [^{11}C]UCB-a as a PET marker for synaptic density in humans. J Nucl Med. 2017;58:631.
14. Bretin F, Bahri MA, Bernard C, Warnock G, Aerts J, Mestdagh N, et al. Biodistribution and radiation dosimetry for the novel SV2A radiotracer [^{18}F]UCB-H: first-in-human study. Mol Imaging Biol. 2015;17:557–64. https://doi.org/10.1007/s11307-014-0820-6.
15. Logan J, Fowler JS, Volkow ND, Wang GJ, Ding YS, Alexoff DL. Distribution volume ratios without blood sampling from graphical analysis of PET data. J Cereb Blood Flow Metab. 1996;16:834–40. https://doi.org/10.1097/00004647-199609000-00008.
16. Cunningham VJ, Rabiner EA, Slifstein M, Laruelle M, Gunn RN. Measuring drug occupancy in the absence of a reference region: the Lassen plot re-visited. J Cereb Blood Flow Metab. 2010;30:46–50. https://doi.org/10.1038/jcbfm.2009.190.
17. Wu Y, Carson RE. Noise reduction in the simplified reference tissue model for neuroreceptor functional imaging. J Cereb Blood Flow Metab. 2002;22:1440–52. https://doi.org/10.1097/01.wcb.0000033967.83623.34.
18. Finnema SJ, Nabulsi NB, Mercier J, Lin SF, Chen MK, Matuskey D, et al. Kinetic evaluation and test-retest reproducibility of [11C]UCB-J, a novel radioligand for positron emission tomography imaging of synaptic vesicle glycoprotein 2A in humans. J Cereb Blood Flow Metab. 2017:271678x17724947. https://doi.org/10.1177/0271678x17724947.
19. Kletting P, Glatting G. Model selection for time-activity curves: the corrected Akaike information criterion and the F-test. Z Med Phys. 2009;19:200–6.

20. Glatting G, Kletting P, Reske SN, Hohl K, Ring C. Choosing the optimal fit function: comparison of the Akaike information criterion and the F-test. Med Phys. 2007;34:4285–92. https://doi.org/10.1118/1.2794176.
21. Golla SSV, Adriaanse SM, Yaqub M, Windhorst AD, Lammertsma AA, van Berckel BNM, et al. Model selection criteria for dynamic brain PET studies. EJNMMI Phys. 2017;4:30. https://doi.org/10.1186/s40658-017-0197-0.
22. Alves IL, Vallez Garcia D, Parente A, Doorduin J, Dierckx R, Marques da Silva AM, et al. Pharmacokinetic modeling of [11C]flumazenil kinetics in the rat brain. EJNMMI Res. 2017;7:17. https://doi.org/10.1186/s13550-017-0265-4.
23. Slifstein M, Laruelle M. Effects of statistical noise on graphic analysis of PET neuroreceptor studies. J Nucl Med. 2000;41:2083–8.
24. Wong K-P, Wardak M, Shao W, Dahlbom M, Kepe V, Liu J, et al. Quantitative analysis of [^{18}F]FDDNP PET using subcortical white matter as reference region. Eur J Nucl Med Mol Imaging. 2010;37:575–88. https://doi.org/10.1007/s00259-009-1293-8.
25. Van Laere K, Ahmad RU, Hudyana H, Dubois K, Schmidt ME, Celen S, et al. Quantification of [^{18}F]JNJ-42259152, a novel phosphodiesterase 10A PET tracer: kinetic modeling and test-retest study in human brain. J Nucl Med. 2013;54:1285–93. https://doi.org/10.2967/jnumed.112.118679.